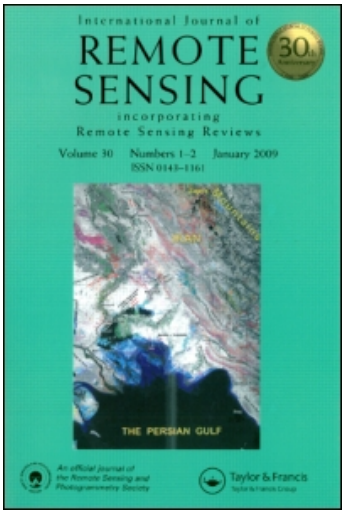

International Journal of Remote Sensing
Publication details, including instructions for authors and subscription information:
http://www.informaworld.com/smpp/title~content=t713722504

Adaptive clustering of airborne LiDAR data to segment individual tree crowns in managed pine forests

H. Lee [a]; K. C. Slatton [ab]; B. E. Roth [c]; W. P. Cropper JR [c]
[a] Department of Electrical and Computer Engineering, University of Florida, Gainesville, FL, USA [b] Department of Civil and Coastal Engineering, University of Florida, Gainesville, FL, USA [c] School of Forest Resources and Conservation, University of Florida, Gainesville, FL, USA

Online publication date: 13 January 2010

To cite this Article Lee, H., Slatton, K. C., Roth, B. E. and Cropper JR, W. P.(2010) 'Adaptive clustering of airborne LiDAR data to segment individual tree crowns in managed pine forests', International Journal of Remote Sensing, 31: 1, 117 — 139
To link to this Article: DOI: 10.1080/01431160902882561
URL: http://dx.doi.org/10.1080/01431160902882561

International Journal of Remote Sensing
Vol. 31, No. 1, 10 January 2010, 117–139

Taylor & Francis
Taylor & Francis Group

Adaptive clustering of airborne LiDAR data to segment individual tree crowns in managed pine forests

H. LEE†, K. C. SLATTON*†‡, B. E. ROTH§ and W. P. CROPPER JR§
†Department of Electrical and Computer Engineering, University of Florida, Gainesville, FL 32611, USA
‡Department of Civil and Coastal Engineering, University of Florida, Gainesville, FL 32611, USA
§School of Forest Resources and Conservation, University of Florida, Gainesville, FL 32611, USA

(*Received 31 December 2007; in final form 4 February 2009*)

Measuring individual trees can provide valuable information about forests, and airborne light detection and ranging (LiDAR) sensors have been used recently to identify individual trees and measure structural tree parameters. Past results, however, have been mixed because of reliance on interpolated (image) versions of the LiDAR measurements and search methods that do not adapt to variations in canopies. In this work, an adaptive clustering method is developed using airborne LiDAR data acquired over two distinctly different managed pine forests in North-Central Florida, USA. A crucial issue in isolating individual trees is determining the appropriate size of the moving window (search radius) when locating seed points. The proposed approach works directly on the three-dimensional (3D) 'cloud' of LiDAR points and adapts to irregular canopies sizes. The region growing step yields collectively exhaustive sets in an initial segmentation of tree canopies. An agglomerative clustering step is then used to merge clusters that represent parts of whole canopies using locally varying height distribution. The overall tree detection accuracy achieved is 95.1% with no significant bias. The tree detection enables subsequent estimation of tree height and vertical crown length to an accuracy better than 0.8 and 1.5 m, respectively.

1. Introduction

Forests are important ecosystems because they strongly modulate stores and fluxes of water and carbon near the Earth's surface. Natural and managed forests also comprise an important renewable resource for the timber and paper industries. Several tree characteristics, such as stem number, density, stem volume, tree height and canopy architecture, are of interest to forest resource managers. These parameters are used to estimate forest yield, describe structural characteristics for wildlife habitat, model future growth and yield, and evaluate the effectiveness of past (and need for future) silvicultural activities. Traditionally, most of these parameters have been measured using direct (*in situ*) field methods. However, traditional ground-based

*Corresponding author. Email: slatton@ece.ufl.edu

International Journal of Remote Sensing
ISSN 0143-1161 print/ISSN 1366-5901 online
http://www.tandf.co.uk/journals
DOI: 10.1080/01431160902882561

forest inventories are expensive and time-consuming and, as a result, are often limited to relatively small sample areas within the landscape of interest.

Efforts have been made to extract information about forests more efficiently using remote sensing methods. The majority of this work to date has used multispectral or microwave (radar) methods. Visual interpretation from high-resolution aerial images (Brandtberg and Walter 1998, Gong *et al.* 2002) is often time-consuming and subjective because the two-dimensional (2D) representation does not possess direct information from below the top canopy layer. Radar methods have the ability to partially penetrate forest canopies and thus can provide some direct information about canopy density and structure (Hyyppä *et al.* 1997, 2000). However, radar-based approaches are typically limited to spatial resolutions at the few metre scale (airborne) or few tens of metres scale (spaceborne), which is too coarse to segment individual trees robustly, making it problematic to estimate tree-based parameters from such data.

Scanning laser ranging technology is well suited for measuring point-to-point distances because of its ability to generate small beam divergences. As a result, many of the laser pulses emitted from airborne light detection and ranging (LiDAR) systems are able to reach the ground underneath the trees through small (10 cm scale) gaps in the canopy. Using high pulse rate lasers and fast optical scanners, airborne LiDAR systems can provide both high spatial resolution and canopy penetration, and these data have become more widely available in recent years for use in environmental and forestry applications (Roth *et al.* 2007b, Slatton *et al.* 2007). Airborne LiDAR sensors directly measure the vertical distribution of the vegetative material above the soil surface and can also be used to provide 3D characterizations of structure. The small-footprint, discrete-return Airborne Laser Swath Mapping (ALSM) system at the University of Florida (UF) is used to acquire elevation measurements with submetre horizontal spacing (15–20 cm location accuracy) and 5–10 cm vertical accuracy over two managed pine forests in North-Central Florida, USA.

Locating and delineating individual tree crowns can enable improved estimates of the height, density and species of trees; crown area and volume; canopy closure; gap fraction; and biomass (Gougeon and Leckie 2003, Reutebuch *et al.* 2005). For the detection of single trees from LiDAR data, most previous work has focused on segmentation of rasterized or interpolated tree canopy models (i.e. 2D digital images that describe the outer contour of the tree crowns) using standard image processing methods (Hyyppä *et al.* 2001, Persson *et al.* 2002, Holmgren and Persson 2004, Chen *et al.* 2006, Koch *et al.* 2006). As airborne LiDAR data are acquired as a discrete set of point locations, a so-called 'point cloud', direct processing on the original LiDAR point data rather than rasterized images is also possible, as reported (Andersen *et al.* 2002, Pyysalo and Hyyppä 2002, Morsdorf *et al.* 2003, Wack *et al.* 2003). Raster formats can be useful for interpolating across voids in the point cloud, particularly when the spatial density of the LiDAR points is not high. However, with the increased spatial density of modern LiDAR data sets, working directly on the point data offers the possibility of estimating characteristics of crown shape and structure from the segmented laser points in three dimensions. When this is done, the LiDAR measurements can be aggregated in a manner that adapts to local 3D (tree-based) geometry rather than in a fixed Cartesian framework. This approach readily accommodates irregular (non-smooth) canopy contours.

By starting with a digital tree height model (DTHM) as the difference between the digital surface model (DSM) and the digital terrain model (DTM), Pyysalo and Hyyppä

(2002) developed a vector polygon model on point clouds to describe canopies and extract tree features, Morsdorf *et al.* (2003) defined the tree locations using the DSM and used k-means clustering in the point data to delineate tree crowns, and Wack *et al.* (2003) defined a cone for the tree top by creating a sorted list of points based on a simple geometry model. In one of the very few attempts to use Bayesian methods on the point data, Andersen *et al.* (2002) proposed a Bayesian object recognition approach to fit ellipsoid crown models to the LiDAR point data. Our approach, however, is to develop an adaptive region growing method that allows us to associate each point with a given tree while avoiding a rigid parametric description of the crown structure. The Bayesian approach allows us to determine the optimal stopping criterion for the point clustering process that minimizes the segmentation error.

There is strong interest in the integration of laser scanning and aerial imagery because laser data provide accurate height information and 3D crown shape (at high point densities), whereas optical imagery provides better planform geometry and colour (spectral) information (Hyyppä *et al.* 2004). Leckie *et al.* (2003), Popescu *et al.* (2003 2004) and Popescu and Wynne (2004) used laser scanning and aerial imagery data on the problem of single tree isolation. However, our focus here was to develop an improved method to segment trees based solely on LiDAR measurements, with the understanding that the proposed method could subsequently be used in conjunction with imagery to further improve segmentation.

The most common approach to segmenting trees in LiDAR data is to use a region growing algorithm instantiated with 'seed points' on each tree. Finding the seeds (i.e. treetops) is a crucial step in the process of detecting individual trees because subsequent steps are heavily dependent on the number of seeds and the locations of seeds. Most current approaches are moderately successful, provided that the filter size and image smoothing parameters are appropriate for the particular tree size and image resolution (Gougeon and Leckie 2003). Finding an appropriate size of filter (or search radius when point data is used) to detect the treetops is not a trivial problem because different filter sizes should be applied to different areas for optimal detection accuracy. Schardt *et al.* (2002) and Brandtberg *et al.* (2003) tried to solve this problem using a linear scale-space method (Lindeberg 1996) that was based on Gaussian smoothing of the rasterized image data at multiple scales. The results from this approach remain sensitive to determining the appropriate scale parameter, and the step of convolving the image with a Gaussian kernel could be problematic because individual canopies may exhibit diverse asymmetric shapes.

In this work, we address the issue of the size of the search radius, R, and propose an approach that automatically grows locally optimal canopy clusters, or regions (equivalent to an adaptive search radius), to segment individual trees. All steps in the process work directly on the 3D 'cloud' of LiDAR points. We first separate the laser returns corresponding to the ground from those corresponding to the above-ground biomass using an adaptive multiscale filter (Kampa and Slatton 2004). In the process, the low order (slowly varying) terrain surface is subtracted from the LiDAR points to 'level out' the ground. The subsequent tree segmentation operates only on the above-ground points and is divided into three main stages: (1) finding all possible seed points for each tree using a minimum search radius $R_{\min}$, (2) region growing instantiated at those seed points, and (3) merging partial tree detections (incomplete clusters) using an agglomerative hierarchical structure. By segmenting the LiDAR points for individual trees, we show it is possible to estimate tree location, tree height and the crown length of each tree. The parameters estimated from the LiDAR data

are compared with ground truth data from a field survey and found to exhibit good accuracy. In §2, we describe the study areas, ground truth measurements and our LiDAR data set. In §3, we present our methodology for segmenting tree canopies, and we present the results in §4. Finally, in §§5 and 6, we discuss the results and present our conclusions.

2. Materials

2.1 *Study sites*

Managed forests comprise an important subset of all forests due to the economic capital invested in them and the resources derived from them. Data were collected from two different managed sites called the Pine Productivity INteractions on Experimental Sites (PPINES; Roth *et al.* 2007a) and the Intensive Management Practices Assessment Centre (IMPAC; Swindel *et al.* 1988, Jokela and Martin 2000) (figure 1). The topography in these North-Central Florida sites is generally very flat, with ground elevations varying by as little as 2 m. The algorithm in this study was developed based on the PPINES data, and subsequently tested on both PPINES and IMPAC. The relevant biophysical parameters and aggregate statistics for the trees in each site are discussed briefly below, with additional information listed in table 1. An example of the spatial tree height distribution from each culture treatment at each site is shown in figure 2. The percentage of living trees (relative to those originally planted) in PPINES is 91.8%, and 65.6% in IMPAC. These data indicate that there can be significant variability in canopy size and morphology between plantations of the same species and even within a single plantation, especially in older plots. An adaptive segmentation approach is therefore needed, even for managed forests, to optimally capture such variations within and across different sites.

2.1.1 PPINES. The PPINES site is located in North-Central Florida (30° 14′ N, 82° 18′ W). The site was established by the Forest Biology Research Cooperative (FBRC), located at UF, in January of 2000. In this work, a total of 16 plots at PPINES were selected where all plots have the same species [loblolly pine (*Pinus taeda* L.)], number of planting positions in the measurement plot (48) and spacing between trees

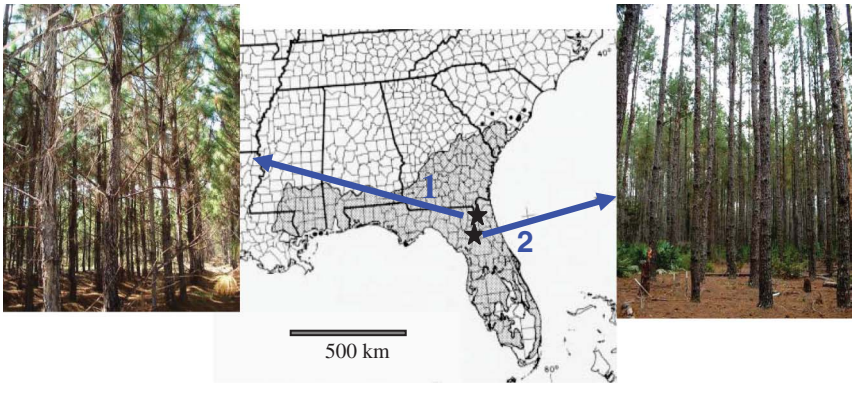

Figure 1. The locations of the study sites (PPINES and IMPAC) with the geographic range of slash pine shaded: (1) the PPINES site, used to develop the algorithm; (2) the IMAC site, used to test the algorithm.

Table 1. February 2006 *in situ* field data from across the study sites describing general information about the sites. The trees at PPINES were 6 years old and those at IMPAC were 23 years old at the time of the investigation. The number of planted trees was 48 in PPINES and 40 in IMPAC for each measurement plot.

Site	Tree species	Treatments	Number of plots	Number of living trees	Tree height (m)	Crown length (m)
PPINES	Loblolly pine	High culture, low culture	16	705	10.7 7.9 4.4	7.9 5.5 2.9
IMPAC	Loblolly pine, slash pine	High culture, low culture	12	315	26.1 21.3 10.0	15.8 6.2 0.9

The tree dimensions (tree height and crown length) are written in the order of the maximum, mean and minimum from the top in each case.

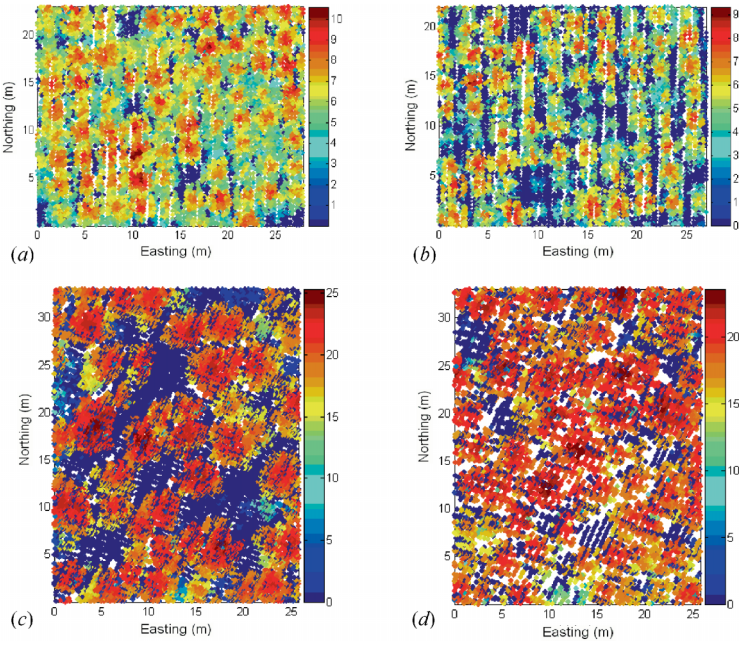

Figure 2. Top view of first-stop LiDAR point heights of a typical plot from each cultural intensity at each site: (*a*) high culture at PPINES; (*b*) low culture at PPINES; (*c*) high culture at IMPAC; (*d*) low culture at IMPAC. All units are in metres. Elevations represent relative heights above the ground. Variable point densities across the LiDAR data sets are primarily due to differences in scan angle.

(2.74 m $\times$ 2.74 m) arranged in six rows (beds) of eight trees each. However, the plots are split into two different culture treatments (high and low). High cultural intensity attempts to maximize growth and health of the growing stock by understorey vegetation control and fertilization. Over the 16 PPINES plots, the trees averaged 7.9 m tall with a live crown length of 5.5 m.

2.1.2 IMPAC. IMPAC is located near Gainesville, Florida (29° 45′ N, 82° 17′ W), and was established in January 1983 with two different species, loblolly pine and slash pine (*P. elliottii* Engelm. var. *elliottii*). A total of 12 plots were sampled consisting of three replicates for each of the species by culture treatment combinations. Each measurement plot was 0.027 ha in size consisting of 40 planting positions on a 3.66 m × 1.83 m spacing arranged in five rows (beds) of eight trees each. Over the 12 IMPAC plots, the average tree height was 21.3 m and the average live crown length was 6.2 m. Due to their advanced stage, the tree stands at IMPAC are at or near maximum carrying capacity, resulting in significant tree mortality in some of the plots. As a result, the number of trees, tree heights and the sizes of canopies at this site vary significantly. Unlike the conical shape of crowns in PPINES, the trees in IMPAC exhibit a wider range of shapes.

2.2 *Collection of field data and LiDAR data*

The nominal positions of individual living trees were available because all planting positions were accurately georeferenced when the plots were established. Ground surveys were performed in February 2006 for both sites to record the tree heights (HT) and the lengths of live crowns (CL). Height to the base of the live crown was measured directly in the field and crown length was then interpreted as the difference between total height and height to the base of the live crown. Locations of leaning trees and very small trees were noted in the ground surveys. Given that planting locations were known, the ground surveys were mainly used to verify the individual tree segmentation results and estimates of HT and CL. High-resolution aerial imagery was used to assist the comparison between the segmentation results and the ground surveys, particularly where leaning trees resulted in crowns not well centred over the trunks, which occurred more in the older IMPAC site. The aerial imagery was acquired by a RedLake MS4100 true colour (RGB)/colour-infrared (CIR) digital camera simultaneously with the LiDAR data from a flying height of 350 m. It was georeferenced to the same coordinate frame as the LiDAR data, and the average ground resolution of the pixels was roughly 10 cm. Since our objective here was to explore the degree to which information can be extracted from LiDAR data to segment trees, we only used the aerial imagery to aid in visual validation and not in the actual segmentation. In locations where the ground survey and aerial imagery indicate a tree is present but the segmentation associates the corresponding LiDAR points with an adjacent tree, that tree is considered 'missed' by the segmentation. This sometimes occurs if a tree is significantly smaller than its neighbours. If, however, a complete tree is indicated by the segmentation algorithm but the ground survey and aerial imagery indicate that the corresponding LiDAR points belong to an adjacent tree, that is considered to be a false positive or 'false tree'.

LiDAR data were collected as close in time to the ground surveys as possible. Collection of *in situ* and remotely sensed data at the same time is always the ideal, but we expect only negligible canopy differences if they are collected during the same year and season. However, considerable canopy changes can generally be expected if measurements are taken during the same season but in a different year, especially if the site has young fast-growing trees, or during different seasons, especially for deciduous trees. The LiDAR data used in this study were acquired by the UF-ALSM system on 9 March 2006. Both the first and the last returns were recorded, and each laser return is the result of laser photons reflecting from the ground or foliage back up to the ALSM receiver

optics. The first returns tend to reflect more from the top canopy, and the last returns reflect more from the understorey and the ground. High laser point densities are generally required to robustly detect individual tree crowns. Given that the maximum available laser pulse rate was 33 kHz for these acquisitions, the flight plans were configured for dense coverage. To achieve high point densities, the LiDAR was acquired from a relatively low Above Ground Level (AGL) altitude of 350 m with a reduced scanner angle range ($\pm 10^\circ$ maximum deviation from nadir) and a 45 Hz scan rate. The maximum allowable scan angle of the sensor is $\pm 20^\circ$, but half that value was used to minimize the possibility of laser pulses passing through multiple trees. The average point densities over the study sites were 14.2 points m^{-2} for PPINES and 10.6 points m^{-2} for IMPAC, but the point density in each plot varied from 12 to 18 points m^{-2} for PPINES and from 8 to 20 points m^{-2} for IMPAC because of variations in overlap among the multiple flight lines and the particular scan angle.

3. Methodology

3.1 *Preprocessing*

Most studies using small-footprint laser altimetry to date have focused on surficial mapping. In those analyses, segmentation algorithms are usually applied to estimate the bare surface elevations by 'filtering out' returns from the vegetation using empirical thresholds on height variance or spatial connectedness of points (Weed *et al.* 2002, Haugerud *et al.* 2003, Zhang *et al.* 2003). We use an adaptive multiscale filter developed by Kampa and Slatton (2004) to separate the laser returns corresponding to the ground from those corresponding to the above-ground biomass. The filter uses an information-theoretic hierarchical data segmentation scheme. First, the area is classified into heavily vegetated and minimally vegetated cells. Then, a Gaussian mixture model (GMM) is estimated from the vertical histogram of aggregated last return points. An asymmetric decision rule is applied to the GMM to ensure that the probability of missing a ground return is less than the probability of erroneously admitting a non-ground return in the bare surface estimate. This decision rule is used to capture small-scale surface features, such as scarps and stream banks. This filter avoids empirical thresholding on the point distributions and retains the 3D 'point cloud' data format. Both study areas are relatively flat, so the terrain slope and height are not a factor for this work. However, to remove the contribution of the terrain slope and heights for arbitrary sites, the low order (slowly varying) terrain surface is subtracted from the LiDAR points to 'level out' the ground.

3.2 *Finding seed locations*

Finding the seed points (i.e. treetops) for canopies in the LiDAR point cloud is a crucial step because it serves as the initial condition for subsequent steps. The search radius R (or, when rasterized image data are used, the window size of the local-maximum filter) determines the minimum allowable canopy radius, and the seed point should be the highest LiDAR point for a particular tree canopy. In this section, an algorithm is developed to find the seed locations using the raw laser point data assuming that R is known for the region of interest (ROI). In general, the appropriate size of R is not known, and this case is explored in §3.3. The elevations of the first-stop LiDAR points are used for this step because these points better express the overall top canopies than do the last-stop elevation points.

To identify the seed points, we start by finding the highest point h_1 in the LiDAR data set, denoted by A, which is taken to be the first seed point s_1. The subset A' is then formed by removing points proximal to s_1 from the set A. Proximal points are defined to be those points in the full data set A inside a circular search region (with the radius R) centred at a seed point. The highest point h_2 is then located within A'. If h_2 is higher than the set of points proximal to h_2 in set A (see figure 3(a)), it is identified as a second seed point s_2 and a reduced subset A'' is defined. If h_2 is not higher than the points proximal to it (see figure 3(b)), we identify the next highest point h_3 in A'. The process is repeated to identify additional seed points in progressively smaller subsets $...A'' \subset A' \subset A$ while using the entire data set A to search for proximal points. This process terminates when all such seed points are found. The seed points are then indexed to represent individual trees.

3.3 *The effect of R on finding seed points*

Most previous algorithms for finding seed points either assume that the search radius R (or size of the moving window) is known *a priori* or they empirically test different sizes to find the best one for a particular site. However, it is not optimal to define a single measure of canopy size because of their irregular shapes and different morphologies across various tree species, ages and management treatments. As would be expected, tree detection results are very sensitive to the size of R. If R is too large, small trees are missed, yet elongate branches (or small clusters of branches) are mistakenly segmented as trees if R is too small (see figure 4). Therefore, there is a need for a systematic approach to find an optimal size for R that automatically adapts to local variations in canopies.

As an example, a small area (14 m × 14 m) in the IMPAC site is selected (see figure 5(a)). Figure 5(b) shows the changes in the number of detected seeds when different sizes of R (from 10 to 1 m in intervals of 0.1 m) are used over the area. Note that using smaller intervals than 0.1 m or R values smaller than 1 m would not provide any reliable improvement because the LiDAR data have approximately decimetre point spacing. Using the algorithm described in §3.2, we see that more trees are detected as R decreases, but we also get more falsely detected trees. There are nine trees in this example area, and the number of detected seed points is very close to the ground truth when $R = 1.3$ m, but it did not find the correct number of trees. The implication is that a single value of R is not sufficient to detect all different sizes of trees in general. To overcome this problem, an agglomerative clustering approach is

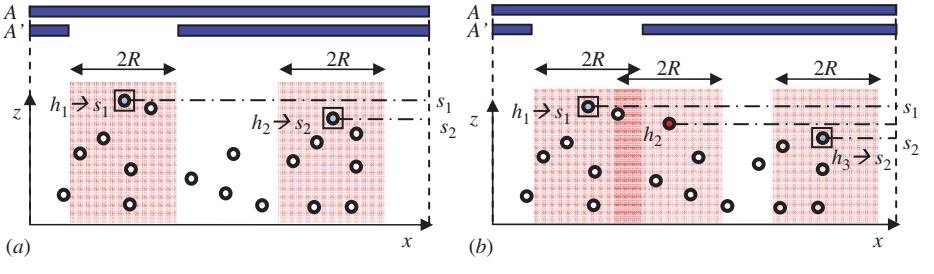

Figure 3. (a) The case of the highest point in set A', h_2, being above all points within the search region ($2R$), so that $h_2 \rightarrow s_2$. (b) The case of the highest point in A', h_2, not being above all points within the search region ($2R$), so $h_3 \rightarrow s_2$.

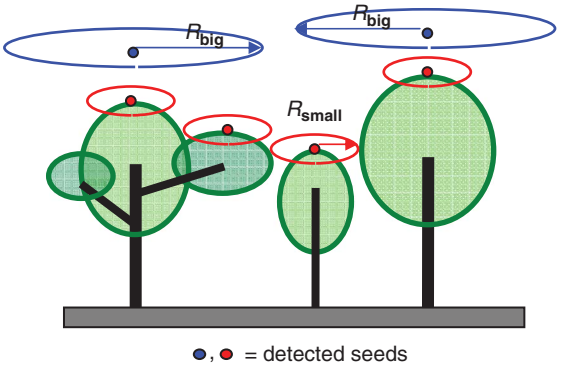

Figure 4. Sensitivity of the detection result to the search region R. If a single R value is used that is too big, elongated branches are not detected as trees but some small trees are missed. The converse occurs if a single value for R is used that is too small.

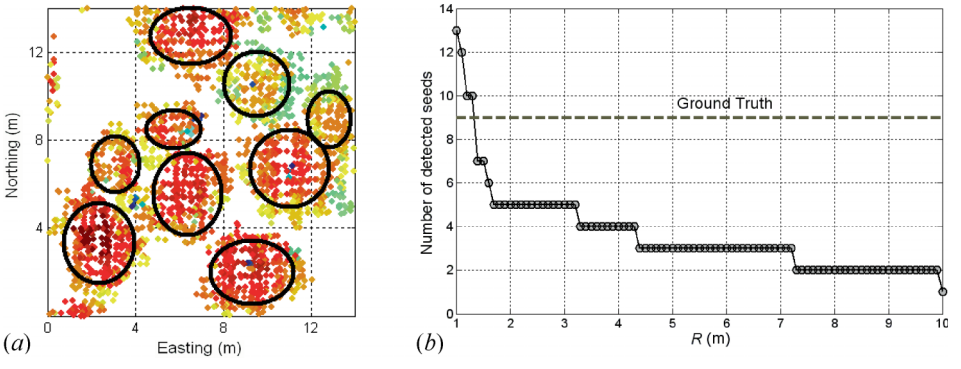

Figure 5. (*a*) The ground truth of a small selected area (14 m × 14 m). The known tree locations are circled in the area. (*b*) The number of detected seeds for the area depending on the size of R. The number of real trees in the plot (nine) is indicated by the dashed line.

developed and described in §3.5. Through the local agglomeration of small clusters, the effect of a spatially adaptive R is realized while ensuring that every point is uniquely associated with a particular tree cluster.

3.4 *Region growing process*

After finding the seed locations, the remaining LiDAR points associated with individual tree canopies need to be delineated. It is challenging to extract the exact boundaries between trees because some tree canopies are intermingled (overlapping in 3D) and tree canopy boundaries are not always distinct. The well-known watershed segmentation algorithm (Beucher and Lantuejoul 1979) has been the most popular method to delineate the tree crown boundaries in 2D (image) data. By conceptually pouring water onto the elevation image starting at the seed locations, the approximate tree boundaries are detected as connected paths. In this study, we develop a new method that is similar in concept to the watershed segmentation but applicable to the raw LiDAR 3D point data.

To find the boundary of each tree, the first-stop elevation points are used. First, the seed points are found using $R = 1$ m and then indexed. Starting from the highest point that is not already indexed, we find the nearest indexed point that is above the current considered point. If the horizontal distance between the current point and that nearest indexed neighbour is smaller than an interval T, the current point is assigned the same index number as that neighbour. Otherwise, it is not labelled. The interval T starts from 0.1 m. Once all the points in the ROI are considered, T is increased by 0.1 m, and the process is repeated. This incremented labelling progressively grows the clusters of LiDAR points associated with each seed point until we form a collectively exhaustive and mutually exclusive collection of sets representing the initial tree canopies. The purpose of restricting the labelling to a neighbourhood, set by T, and adopting the label of the nearest indexed point within that neighbourhood regardless of whether it is a seed point or just a previously indexed point is to reduce the chance of erroneously associating a considered point on a large canopy with a smaller tree (seed) that happens to be closer. The LiDAR point spacing dictates the range of reasonable starting values and step sizes for T, which are roughly 1 to 2 times the nominal LiDAR point spacing. An example of a region growing result is shown in figure 6. In this, the seed points were found using $R = 1$ m, and the regions were subsequently grown by incrementing T from 0.1 m in steps of 0.1 m until all points were labelled.

3.5 *Agglomerative hierarchical clustering*

Even with the incremented labelling described in §3.4, we expect the initial results to be oversegmented in some instances (as seen in figure 6) because R was chosen small so as not to miss trees. An agglomerative hierarchical clustering approach is therefore used to overcome this oversegmentation. Agglomerative hierarchical methods generally begin with each observation being considered as a separate cluster and then proceed to combine clusters until all observations belong to one cluster or some stopping criterion is satisfied. Each LiDAR point could represent an individual observation (i.e. singleton) in the lowest level of the hierarchical clustering data structure, but it would not be very meaningful or computationally efficient to use individual LiDAR

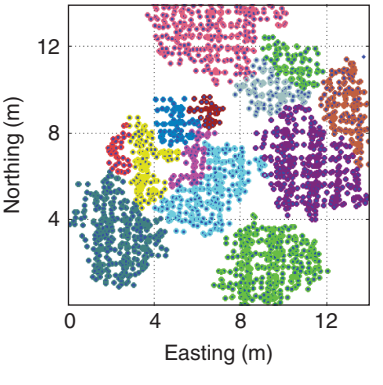

Figure 6. An example of the region growing result with incrementing T from 0.1 m in steps of 0.1 m until all points were labelled. The seed points were found using $R = 1$ m. This is a downward-looking view of the area in figure 5. Each colour indicates a segmented cluster of LiDAR points representing a detected tree in the region growing process. Oversegmentation can be seen in some cases.

points to initiate the clustering. As the size of R dictates the size of tree canopy clusters that can be detected, we specify a minimum value for R to be 1 m because no trees smaller than that are present in our study sites. Note, however, that the minimum value of R could be chosen to be smaller if necessary.

The region growing process in §3.4 provides the set of clusters at the lowest level (i.e. the leaf level) of the hierarchical clustering tree. From that point on, clusters are merged solely using agglomeration and not region growing. Small clusters representing partial canopies are merged with their nearest-neighbour cluster in space as determined by the distance $d(r,s)$ between cluster centroids (also known as the 'centroid linkage' method). Essentially, $\min(d)$ is used to establish which clusters are nearest neighbours. In equation (1), $d(r,s)$ is the horizontal l^2-norm (Euclidean distance) between cluster centroids, n_r and n_s are the number of LiDAR points in clusters r and s, respectively, and $\underline{x}_{r_i}$ is the ith point in cluster r.

$$d(r,s) = \left\| \frac{1}{n_r} \sum_{i=l}^{n_r} \underline{x}_{r_i} \frac{1}{n_s} \sum_{i=l}^{n_s} \underline{x}_{s_i} \right\|_2 \tag{1}$$

In most agglomerative methods, the decision to merge clusters requires a threshold test on a similarity measure. For tree segmentation, when attempting to select a threshold value based solely on 2D measures of horizontal point similarity, it is generally not possible to find a value that provides good separation among all trees and yet does not oversegment individual tree canopies that exhibit large elongated branches (i.e. partial-tree clusters), which may appear similar to small, yet complete, tree clusters. Thus, we exploit the canopy penetration of the LiDAR to find a threshold based upon vertical point adjacency within a cluster. A value for each cluster is assigned to be the standard deviation of z values (above-ground elevations of both first and last returns),σ_z. It was suspected that high values of σ_z would occur for complete trees and lower values of σ_z would occur for elongated branches because of the larger vertical distribution of biomass in complete trees. All clusters satisfying $\sigma_z < \tau$ are merged with their nearest cluster neighbours by the centroid linkage technique, where the threshold τ is determined by supervised learning. This process is repeated at the next level in the clustering tree until no clusters remain with $\sigma_z < \tau$ Through this process, we realize the effect of a spatially adaptive R.

To determine the threshold, τ, a Bayesian approach was used with 120 training sample points randomly selected from each class (partial tree clusters w_1 and complete tree clusters w_2) at the PPINES site. The training samples for each class were chosen manually by using the initial region growing results, as shown in figure 6. Using the ground surveys and aerial images, training samples were unambiguously labelled as belonging to either class w_1 or class w_2. The conditional probability density function (pdf) for each class (i.e. the likelihood of w_i with respect to a given feature x), is non-parametrically estimated using the Parzen windowing approach (Duda *et al.* 2001) and shown in figure 7. The likelihood $P(x|w_i)$ shows the probability of obtaining a particular feature value x (here, $x = \sigma_z$) given that it belongs to class w_i. The optimal (Bayesian) decision boundary between the two classes, x^*, is selected by minimizing the probability of error (equation (2)) under the assumption of equal prior probabilities [i.e. $P(w_1) = P(w_2)$]. Basically, we minimize the probability of error by choosing the maximum *a posteriori* probability. That is, by deciding w_1 if $P(\mathrm{w_1|x}) > P(\mathrm{w_2|x})$ and by deciding w_2 otherwise for a given x. From 100 different subsets of training samples, we observed that the value of x^* was not very sensitive to the particular

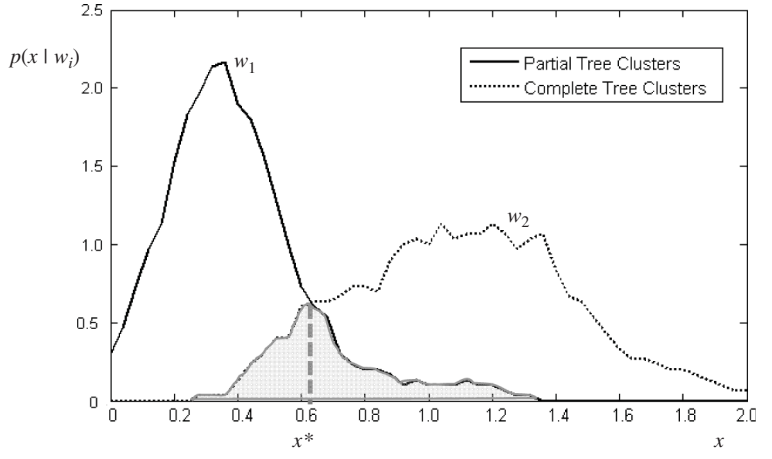

Figure 7. Probability density functions of the two classes (w_1: partial tree clusters, w_2: complete tree clusters) estimated by the Parzen windowing method. The Bayesian (optimal) decision boundary, x^*, and the resulting probability of error (shaded area) are shown. Here, the random variable x represents the standard deviation (in metres) of heights in the cluster points, σ_2.

training samples. We obtained a mean value of 0.62 for x^*, with a standard deviation of only 0.04. The value of 0.62 was subsequently adopted for τ and used on all plots in both the PPINES and IMPAC study sites.

$$x^* = \underset{-\infty \le x \le \infty}{\text{Arg}} \min[P(\text{error})] \tag{2}$$

where $[P(\text{error})] = P(w_2) \int_{-\infty}^{x} p(x|w_2)\mathrm{d}x + p(w_1) \int_{x}^{\infty} p(x|w_1)\mathrm{d}x$

3.6 *Tree-based parameter estimation*

Once individual trees are detected, the possibility is opened up to estimate important parameters such as the number density of trees, tree height, crown length and crown area directly from the segmented points. From these parameters, other forest parameters, such as diameter at breast height (DBH), basal area and leaf area index (LAI) could be estimated from allometric equations (Amaro *et al.* 2003, Song 2007). Our main objective here was to develop a methodology to accurately segment individual trees from LiDAR data, so we focus on two parameters for which we had *in situ* measured values from a ground survey, namely HT and CL.

3.6.1 HT. The highest point among the segmented points for each tree is considered as the tree top, and the distance to the tree top from the ground is regarded as the height of that tree. Tree heights are commonly underestimated in LiDAR studies (Nilsson 1996, Magnussen *et al.* 1999, Persson *et al.* 2002, McCombs *et al.* 2003) because the transmitted laser pulses may miss the actual tree top. Increasing the spatial density of LiDAR points provides a better chance of hitting the tree top, resulting in better accuracy. It should be noted, however, that even a high LiDAR point density may not completely eliminate a slight underestimation of tree heights, especially from sharp conical shaped crowns, because of the range averaging effect (Lefsky *et al.* 2002). This is the phenomenon in which the maximum elevation registered for a tree corresponds to a height below the top-most branch because the

number of reflected photons required to trigger the receiver electronics may not be achieved until the transmitted pulse encounters more than one branch (Hopkinson 2007). The precise magnitude of this underestimation is difficult to quantify because it can vary with incidence angle, beam divergence, tree species, flying altitude, and the sensitivity of the LiDAR receiver electronics. The nominal height error from UF-ALSM measurements of exposed ground is at the decimetre scale (Shrestha *et al.* 1999), and the errors in the estimation of bare-surface ground elevations underneath forest canopies rarely exceeds 2 or 3 dm (Cho and Slatton 2007).

3.6.2 CL. When conducting field work, foresters are generally interested in an 'effective' CL. A whorl is a common feature of pine trees and is defined as a cluster of branches that radially emanate from the main trunk at roughly the same height. The base of the live crown can be defined as the lowest whorl with 50% or more of the branches containing live green needles. As a tree ages, the older (lower) whorls become shaded by the newer whorls on that tree. This trend is emphasized in managed forests where all trees are at the same stage, so shading on older whorls by neighbouring trees of similar heights increases with time. Whorls die as they age and lose sun exposure, and over time the base of the live crown moves up as the HT increases (Long *et al.* 2004). CL is traditionally determined in the field by subtracting the height to the base of the live crown (HTLC) from the HT. As the loss of live needles can occur over the lower few whorls, it is not always obvious from visual ground inspection precisely which whorl corresponds to the HTLC (Sprinz and Burkhart 1987). As a result, HTLC determined from field surveys can contain bias and uncertainty that are not insignificant.

Attempts have been made to estimate the elevation of the base of the live crown using airborne LiDAR data (Holmgren and Persson 2004, Andersen *et al.* 2005, Popescu and Zhao 2008). It is often problematic, however, because the lower extent of the live canopy is obscured in the point cloud when LiDAR pulses hit stems (trunks) and dead branches. Furthermore, the lower reaches of the live crowns are significantly occluded by the upper portions when canopies are closed, thus reducing the LiDAR points available for sensing the live crown base. In this work, because of the absence of understorey vegetation, a simple method for estimating the height of the live crown base on each tree is developed. This method is intended to be simple enough to require no training and to demonstrate the sort of tree-based parameters that can be estimated once individual trees are segmented in the LiDAR data. It is not necessarily optimal. By smoothing the vertical distribution of non-ground LiDAR points (both first and last returns), the height where a significant number of points first appear in a given tree cluster can be found. A 2-m-long sliding window was incremented up from the ground in 1 m intervals at each tree cluster, and the number of points in the window is counted. When the number of points in the window first exceeds more than 1% of the total number of points in that cluster, the median height of the LiDAR points in the window is recorded as the HTLC of that tree.

4. Results

4.1 *Tree detection*

The results of the tree segmentations are presented in table 2. As shown in figure 2, the canopy distributions differ according to the cultural treatments and the age of the plots, and we expect the segmentation results to be dependent on these distributions.

Table 2. The results of individual tree segmentation. High cultural intensity attempts to maximize growth and health of the trees through fertilization and control of understorey vegetation. Low cultural intensity does not.

					Results			
Site	Plot type	Number of plots	Number of planted trees	Number of living trees	Detected*	Correct†	Wrong‡	Missed§
PPINES	High culture	8	384	351	367	340 (96.9)	27	11
	Low culture	8	384	354	356	349 (98.6)	7	5
IMPAC	High culture	6	240	134	150	129 (96.3)	21	5
	Low culture	6	240	181	154	152 (84.0)	2	29
Total	–	28	1248	1020	1027	970 (95.1)	57	50

*The number of all trees detected by the algorithm.
†The number of trees that are correctly detected among all detected trees; their percentages are given in parentheses.
‡The number of trees detected by the algorithm that do not exist in the ground truth (partial canopies labelled as whole trees).
§The number of trees that the algorithm could not detect (whole trees labelled as partial canopies and subsequently merged into nearest complete trees).

The evaluation of the tree detection was based on the measurement plots even though the algorithm detects all the trees inside the treatment plots. The areas on all sides in the treatment plots but not in the measurement plots comprise a buffer zone that mitigates edge effects in the spatial analysis.

The overall detection accuracy was 970/1020 = 95.1%. The number of false positives (57 trees) was similar to the number of false negatives (50 trees), suggesting no overall bias. As expected, the detection accuracy was higher at PPINES because the horizontal distribution of trees was more regular due to their young age and square spacing. It is interesting to note that the average height of the missed trees was 17.92 m at IMPAC and 7.56 m at PPINES, while the average ground truth tree height was 21.34 m at IMPAC and 7.94 m at PPINES. The fact that the average missed tree was shorter than the average tree at IMPAC and at PPINES indicates that the LiDAR measurement and subsequent segmentation are slightly more likely to miss the smaller trees than the larger trees. While this tendency is not unexpected, the bias with respect to tree height is not unduly large and is partially due to the irregular canopy shapes and sizes at IMPAC. This suggests that the algorithm is fairly robust over a range of tree heights and canopy sizes. The plots at the PPINES with low culture showed the best result (98.6%) without significant bias. In the high culture plots, the trees grew larger, resulting in more overlap and complexity in the canopy distributions. This caused more occurrences of 'Wrong' and 'Missed', but the percentage of correctly detected trees (96.9%) was still close to that of the low culture plots. The detection results at the IMPAC plots with high culture were as good as the high culture results at PPINES because fertilization made the older trees at IMPAC larger and distinct from their neighbours. Also contributing to this high detection accuracy was the fact that fertilization over the long duration of the IMPAC plots eventually resulted in instances of competitive tree mortality (see table 2), which increased some of the gaps between trees. The lowest detection accuracy occurred for the case of the low culture plots at IMPAC (84.0%). Unlike at PPINES, the IMPAC plots with low culture had less tree mortality (more closely packed trees) and more irregularity in canopy size and shape. Several difficult cases were also observed in these plots where small trees were leaning towards nearby taller trees and parts of their canopies were underneath or inside neighbouring trees.

A segmentation result on a plot at the PPINES with high culture is shown in figure 8. Odd-shaped tree canopies are successfully detected because no assumptions are made on horizontal canopy morphology. The tree top, tree boundary and LiDAR points of each tree are shown in the figure. Two false positives and one false negative are found in the measurement plot.

4.2 *Tree-based parameters*

From the IMPAC site, we were able to use all trees in the 12 plots to estimate HT and CL because the ground truth survey included all trees. It was thus possible to examine two cases for IMPAC. In the first case (case 1), only correctly detected trees are used; that is, falsely detected trees and missed trees are not counted. In the second case (case 2), all trees segmented by the algorithm are used for the experiment. Case 2 is more general as it is not always known beforehand whether a segmented tree is classified correctly or not. Unfortunately, at PPINES only 25% of the trees in each plot (except two plots) were selected to measure the parameters during the ground survey. Therefore, at PPINES, we used all correctly detected trees (83 trees) in two

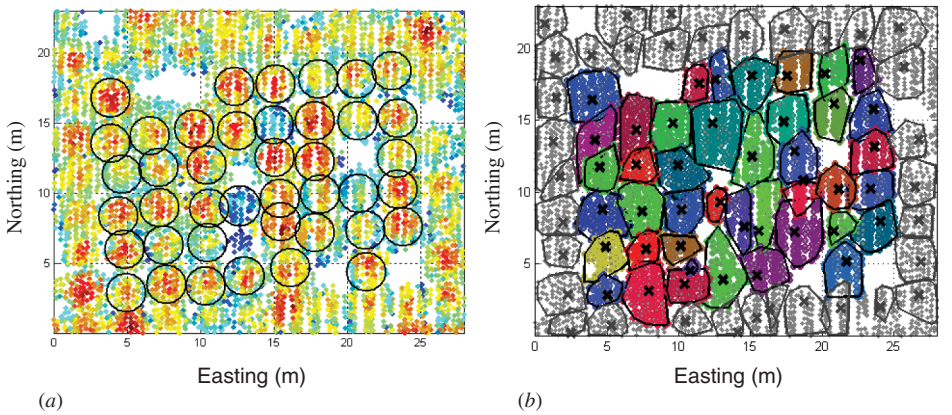

Figure 8. An example of the segmentation results (a plot with high culture at PPINES). (*a*) Known tree locations are circled on top of the first-stop elevation points where the ground points are filtered out. Actual sizes and shapes of the tree canopies are different from those of the circles. (*b*) The segmentation result. A uniform colour is used to indicate the set of LiDAR points that are segmented as a given tree inside the measurement plot. The seed points are marked as crosses and the maximal boundary of each tree is indicated by convex hulls (closed black curves). Detected trees that lie outside the measurement plot are shown with grey crosses and lines.

plots and a random sampling of 140 correctly detected trees from the remaining 14 plots. As a result, wrongly detected trees and missed trees could not be included in the PPINES results. The differences between estimates and ground truth values for HT and CL are summarized in table 3. In figure 9, LiDAR-estimated HT and CL are plotted against field-measured HT and CL for correctly detected trees at both IMPAC and PPINES. Simple linear regression is used to fit the line to each data. Over the range of LiDAR point densities examined here (10–20 points m^{-2}), the root mean square (RMS) errors in the estimates decreased with increasing point density for both the HT and CL (roughly 0.5 to 0.1 m for HT and 1.1 to 0.3 m for CL for 10 to 20 points m^{-2}, respectively).

Table 3. The mean differences between the ground truth values and the estimates of tree height (HT) and crown length (CL). The standard deviations are given in parentheses. As the ground survey at IMPAC was exhaustive, two different cases could be studied: (1) case 1: only correctly detected trees are used; (2) case 2: all trees segmented by the algorithm are used. Only case 1 could be studied at PPINES because the ground survey was based on randomized sampling rather than exhaustive.

	HT (m)			CL (m)		
		Case 2			Case 2	
	Case 1	Whole	Each plot	Case 1	Whole	Each plot
PPINES	0.34 (0.29)	–	–	0.84 (0.58)	–	–
IMPAC	0.78 (0.63)	0.58	0.60 (0.44)	1.40 (0.97)	0.39	0.81 (0.69)

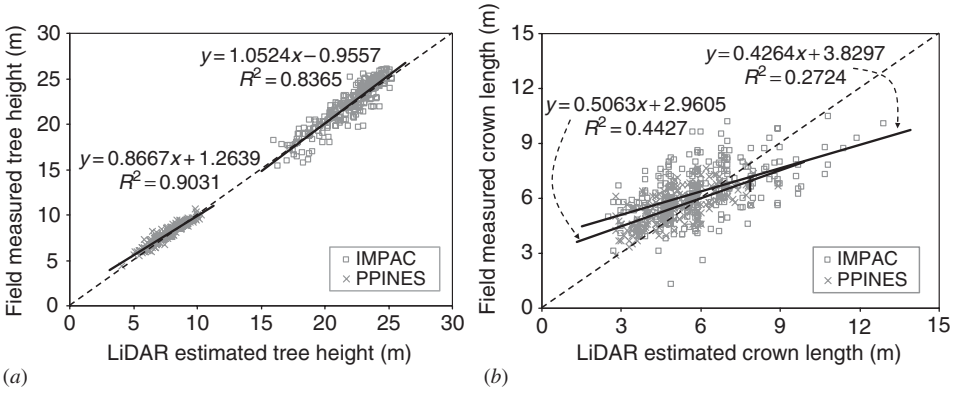

Figure 9. Field measures vs. LiDAR estimates for correctly detected trees at the study sites: (*a*) tree heights; (*b*) crown lengths. The dotted line represents a hypothetical 1:1 ratio between measured and estimated.

4.2.1 HT. For the PPINES site, the mean of all ground truth HT was 7.94 m, and the mean of all estimated HT was 7.71 m. The mean of absolute height differences between the ground truth and the estimates was 0.34 m (percentage of error = ± 4.22%) and the standard deviation was 0.29 m.

For all correctly detected trees in IMPAC (i.e. case 1), the mean of all ground truth HT was 22.00 m, and the mean of all estimated HT was 21.85 m. The mean of absolute height differences was 0.78 m (percentage of error = ± 3.55%) and the standard deviation of them was 0.63 m. For case 2, over the whole (all 12 plots), the mean of all ground truth HT was 21.34 m and mean of all estimated HT was 21.92 m. Of note, this difference (0.58 m) was smaller than the difference achieved in the first case. This shows that there is a good agreement between the mean of all ground truth and the mean of all estimates (from all detected trees) at this site even though the algorithm misses some trees and detects some false trees. To look at a smaller size of the ROI, the same experiment was executed for individual plots (0.027 ha), and the result still shows good agreement but slightly larger errors; the mean of differences between ground truth and estimates of each of the 12 plots was 0.60 m and the standard deviation was 0.44 m. Although it is possible in general for large errors to occur locally, these results imply that good average agreement with ground truth could reasonably be expected even over small plots, such as these.

4.2.2 CL. For the PPINES site, the mean of all ground truth CL was 5.51 m, and the mean of all estimated CL was 5.04 m. The mean of absolute CL differences between the ground truth and the estimates was 0.84 m and the standard deviation was 0.58 m.

For IMPAC, in case 1, the mean of all ground truth CL was 6.39 m, and the mean of all estimated CL was 6.01 m. The mean of absolute CL differences was 1.40 m and the standard deviation was 0.97 m. In case 2, the mean of all ground truth CL was 6.18 m and mean of all estimated CL was 5.79 m. As in the HT estimation, this difference (0.39 m) is smaller than the difference in case 1, showing that there is a good agreement between the mean of all ground truths and the mean of all estimates over the test area. When looking at individual plots, the mean of differences between ground truth and estimates of each of the 12 plots was 0.81 m and the standard deviation was 0.69 m.

Figure 9(*b*) suggests that we tend to underestimate CL for short crowns and overestimate it for longer crowns. The trend appears for both sites, but is slightly more pronounced for IMPAC. Given that HT estimates agree well with field measurements and that CL is taken to be HT minus HTLC, the low correlation in CL is apparently due to a disagreement between the measured and estimated HTLC. As discussed in §3.6, HTLC is a difficult parameter to measure in the field for loblolly and slash pines because of the inherent ambiguity in determining the highest whorl that fails to meet the 50% live needle criterion. In our estimation of CL from the LiDAR data, we used a simple 1% criterion for the vertical distribution of the LiDAR points in each tree cluster. A simple criterion like this is not expected to be optimal. Rather, it is chosen to avoid the need for training an adaptive CL estimator, which is beyond the scope of this paper.

5. Discussion

Using the proposed approach, we obtained overall tree detection accuracies in excess of 95% over the two test sites (see table 2). The only exception was the set of low culture treatment plots at IMPAC, where a fairly good detection accuracy of 84% was still achieved. As mentioned in the previous section, those plots exhibited considerable intermingling among adjacent canopies and greater variation in canopy size and shape. The small standard deviation in x^* across multiple randomized samplings of the training data suggests that our parameterization in the clustering step is robust and could be applied to other managed sites of different tree ages, stem spacings or species using only modest amounts of training data.

5.1 *Parameter estimation*

In the subsequent parameter estimation, we also obtained agreement between estimates and ground truth to within several decimetres. The average HT was underestimated by 0.24 and 0.15 m over PPINES and IMPAC, respectively. Much of this residual is probably caused by instances where the LiDAR did not hit the top-most point of some crowns. There was more chance of missing the treetops over PPINES because the peaks of the crowns tended to be sharper over PPINES than over IMPAC, resulting in larger underestimation for HT over PPINES. The average CL was underestimated by 0.47 and 0.38 m over PPINES and IMPAC, respectively. The slightly larger estimation error for CL is not surprising because CL estimates depend on both the estimated HT and how well the lower canopy is sampled. The occluding effect of the upper canopy implies that the lower canopy is not sampled as densely as the upper canopy. The underestimate of CL at PPINES was slightly larger than at IMPAC. This is probably because the younger tree canopies in PPINES are shorter and thicker resulting in less penetration of the LiDAR. Furthermore, there is always some uncertainty in the field measurements themselves because of irregularities in the terrain surface and measurement errors. In these study sites, the terrain is fairly flat, so any errors that may be present in the ground surveys are most probably due to random measurement errors by field personnel.

Finally, it should also be noted that, based on the segmented LiDAR points, estimates of the vertical projection of maximal crown area for each segmented tree could be obtained using the circumscribing convex hulls computed for each crown cluster (as shown in figure 8(*b*)). Similarly, the 3D shape of the upper crown 'surface' of each tree could be estimated because the LiDAR points provide height information along with horizontal positions. However, we do not present formal estimates of

crown area or shape here as they were not independently measured in the ground survey.

5.2 *Impact of LiDAR point density*

The changes in RMS errors in the estimates of HT and CL over the range of LiDAR point densities reported in §4.2 suggest that high LiDAR point densities are important for accurate estimation of individual tree parameters. In particular, as mentioned in the previous section, higher point densities increase the chances of a LiDAR return from the highest point in each tree canopy, thus reducing underestimation of HT. It would be interesting to determine minimal LiDAR point densities that could still yield useful estimates in order to acquire LiDAR data most efficiently. However, general statements along those lines are problematic because the degree to which lower LiDAR point densities would be useful would depend on the flight pattern (presence of orthogonal flight lines), forest type, parameters being estimated, and the tolerance for uncertainty for the particular application.

5.3 *Data acquisition (flight directions)*

Flying multiple times over a particular ROI is generally necessary to obtain high densities of laser points (10–20 points m^{-2}) given the current constraints on minimum flight speed, minimum allowable flying altitude, maximum laser pulse rate and maximum scanner frequency. Although increasingly high laser pulse rates of new LiDAR systems can reduce somewhat the need for multiple flight lines (Slatton *et al.* 2007). Unlike the flights over IMPAC, only horizontal (East–West) flights were acquired over PPINES. As shown in figure 10, this resulted in narrow vertical (North–South) gaps that are visible in the point clouds between scan lines. While the overall tree

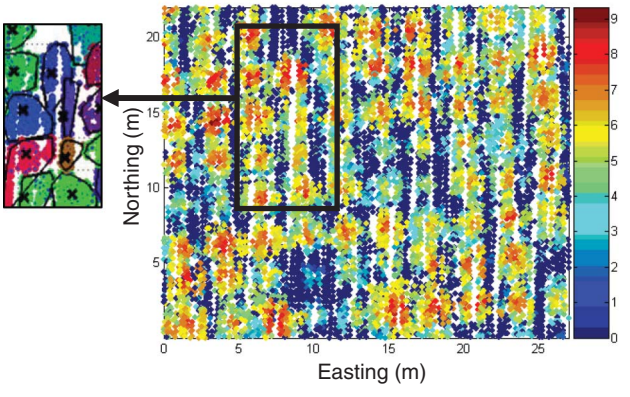

Figure 10. A top view of the low culture PPINES plot shown in figure 2. The aircraft was flying East–West (right–left in the figure) over the site. Narrow gaps roughly 1 m or less in width are visible (marked with a rectangle) in the point data between scan lines even though partially overlapping flight lines were acquired. A subset of the detection result is shown inside the small box to the left. While such gaps do not seem to strongly affect the correct detection of the trees, they can affect the estimated shapes of the detected canopies and estimates of HT and CL in cases where the highest points on the trees are missed. Orthogonal flight lines could mitigate such gaps.

detection accuracy was high despite this phenomenon, in general such gaps can cause difficulty in detecting trees if a tree happens to be separated into a multiple clusters by a gap. The worst case scenario would be when the scan lines from multiple flights overlap almost exactly rather than one flight 'filling in' the gaps from another. Therefore, when researchers have input on the design of the flight plan, orthogonal flight lines should be requested to get better coverage over the ROI.

6. Conclusions

Small footprint LiDAR technology can provide spatially dense coverage over forest canopies and penetrates the canopy by illuminating the ground and understorey through small gaps in the crown layer. These advantages play an important role in allowing the identification of individual trees and estimation of their heights and crown lengths from such LiDAR data. Determining the optimal window sizes to accurately find treetops has been the most important and difficult part in the process of delineating single trees to date. An adaptive region growing method was developed by using an agglomerative hierarchical clustering structure to merge the partial-tree clusters that are segmented by the region growing process.

The stopping criterion on the agglomeration was determined by minimizing the Bayes error over the training data, resulting in a threshold τ. The small standard deviation in τ values obtained from repeated randomized sampling in this study suggests that conditioning the agglomeration on the standard deviation of point elevations is robust and that modest amounts of training data will suffice to estimate τ. To achieve optimal results over sites other than those examined here (particularly if those sites contain tree species other than loblolly and slash pine), the algorithm should be trained using local ground truth data, as described here. Additional features could, in principle, be incorporated for the estimation of τ, but that would be likely to make the results more sensitive to the specific training data set.

The entire process of the proposed approach was developed directly on the raw point cloud data. This method readily accommodates irregular (non-smooth) canopy contours, and avoids rigid parametric descriptions of the canopy shapes and statistics. Working on point data with high point density requires more computational time and/or memory than working with images, but this could be alleviated by dividing the ROI into small areas ('divide-and-conquer' strategy). It was shown that the proposed algorithm performs very well overall for two managed pine plantation forests of different ages and species. The lowest detection accuracy occurred for the IMPAC plots with low culture because the canopies in these plots are more interlocked and more variable in size than in other plots. The average estimates of tree heights and crown lengths were slightly underestimated, but agreed with ground truth to within several decimetres.

Acknowledgements

This work was partially supported by the National Science Foundation (NSF) through the National Centre for Airborne Laser Mapping (NCALM) under grant EAR-0518962 and the US Army Research Office (ARO) under grant W911NF-06-1-0459. We are grateful for the assistance of the Forest Biology Research Cooperative (FBRC) in providing the *in situ* data. Special thanks to Rayonier Inc. and to Drs Eric Jokela and Timothy Martin who provided access to the experimental study sites.

References

Amaro, A., Reed, D. and Soares, P., 2003, *Modelling Forest Systems* (Cambridge, MA: CABI Publishing).

Andersen, H., Reutebuch, S.E. and Schreuder, G.F., 2002, Bayesian object recognition for the analysis of complex forest scenes in airborne laser scanner data. *International Archives of the Photogrammetry, Remote Sensing and Spatial Information Sciences*, **34**, pp. 35–41.

Andersen, H.E., McGaughey, R.J. and Reutebuch, S.E., 2005, Estimating forest canopy fuel parameters using lidar data. *Remote Sensing of Environment*, **94**, pp. 441–449.

Beucher, S. and Lantuejoul, C., 1979, Use of watersheds in contour detection. In *International Workshop on Image Processing: Real-time Edge and Motion Detection/Estimation*, Rennes, France.

Brandtberg, T. and Walter, F., 1998, Automated delineation of individual tree crowns in high spatial resolution aerial images by multiple-scale analysis. *Machine Vision and Applications*, **11**, pp. 64–73.

Brandtberg, T., Warner, T.A., Landenberger, R.E. and McGraw, J.B., 2003, Detection and analysis of individual leaf-off tree crowns in small footprint, high sampling density lidar data from the eastern deciduous forest in North America. *Remote Sensing of Environment*, **85**, pp. 290–303.

Chen, Q., Baldocchi, D., Gong, P. and Kelly, M., 2006, Isolating individual trees in a savanna woodland using small footprint LIDAR data. *Photogrammetric Engineering and Remote Sensing*, **72**, pp. 923–932.

Cho, H. and Slatton, K.C., 2007, Morphological processing of severely occluded digital elevation images to extract and connect stream channels. *IEEE International Conference on Image Processing (ICIP)*, **2**, pp. 241–244.

Duda, R.O., Hart, P.E. and Stork, D.G., 2001, *Pattern Classification*, 2nd edn (USA: John Wiley & Sons), pp. 164–168.

Gong, P., Sheng, Y. and Biging, G.S., 2002, 3D model-based tree measurement from high-resolution aerial imagery. *Photogrammetric Engineering and Remote Sensing*, **68**, pp. 1203–1212.

Gougeon, F.A. and Leckie, D.G., 2003, *Forest Information Extraction from High Spatial Resolution Images using an Individual Tree Crown Approach*. Information Report BC-X-396, Pacific Forestry Centre, Canadian Forest Service, Victoria, BC, Canada.

Haugerud, R.A., Harding, D.J., Johnson, S.Y., Harless, J.L., Weaver, C.S. and Sherrod, B.L., 2003, High-resolution LiDAR topography of the Puget lowland, Washington – a bonanza for earth science. *GSA Today*, **13**, pp. 4–10.

Holmgren, J. and Persson, A., 2004, Identifying species of individual trees using airborne laser scanning. *Remote Sensing of Environment*, **90**, pp. 415–423.

Hopkinson, C., 2007, The influence of flying altitude and beam divergence on canopy penetration and laser pulse return distribution characteristics. *Canadian Journal of Remote Sensing*, **33**, pp. 312–324.

Hyyppä, J., Hyyppä, H., Inkinen, M., Engdahl, M., Linko, S. and Zhu, Y.H., 2000, Accuracy comparison of various remote sensing data sources in the retrieval of forest stand attributes. *Forest Ecology and Management*, **128**, pp. 109–120.

Hyyppä, J., Hyyppä, H., Litkey, P., Yu, X., Haggrén, H., Rönnholm, P., Pyysalo, U., Pitkänen, J. and Maltamo, M., 2004, Algorithms and methods of airborne laser-scanning for forest measurements. *International Archives of the Photogrammetry and Remote Sensing Sciences*, **36**, pp. 82–89.

Hyyppä, J., Kelle, O., Lehikoinen, M. and Inkinen, M., 2001, A segmentation-based method to retrieve stem volume estimates from 3-D tree height models produced by laser scanners. *IEEE Transaction on Geoscience and Remote Sensing*, **39**, pp. 969–975.

Hyyppä, J., Pulliainen, J., Saatsi, A. and Hallikainen, M., 1997, Radar-derived forest inventory by compartments. *IEEE Transaction on Geoscience and Remote Sensing*, **35**, pp. 392–404.

Jokela, E.J. and Martin, T.A., 2000, Effects of ontogeny and soil nutrient supply on production, allocation, and leaf area efficiency in loblolly and slash pine stands. *Canadian Journal of Forest Research*, **30**, pp. 1511–1524.

Kampa, K. and Slatton, K.C., 2004, An adaptive multiscale filter for segmenting vegetation in ALSM data. *IEEE International Geoscience Remote Sensing Symposium (IGARSS)*, **6**, pp. 3837–3840.

Koch, B., Heyder, U. and Weinacker, H., 2006, Detection of individual tree crowns in airborne lidar data. *Photogrammetric Engineering and Remote Sensing*, **72**, pp. 357–363.

Leckie, D.G., Gougeon, F.A., Hill, D.A., Quinn, R., Armstrong, L. and Shreenan, R., 2003, Combined high-density lidar and multispectral imagery for individual tree crown analysis. *Canadian Journal of Remote Sensing*, **29**, pp. 633–649.

Lefsky, M.A., Cohen, W.B., Parker, G.G. and Harding, D.J., 2002, LiDAR remote sensing for ecosystem studies. *BioScience*, **52**, pp. 19–30.

Lindeberg, T., 1996, Scale-space: a framework for handling image structures at multiple scales. Technical Report, CVAP-TN1S, Royal Institute of Technology, Stockholm, Sweden.

Long, J.N., Dean, T.J. and Roberts, S.D., 2004, Linkages between silviculture and ecology: examination of several important conceptual models. *Forest Ecology and Management*, **200**, pp. 249–261.

Magnussen, S., Effermont, P. and LaRiccia, V.N., 1999, Recovering tree heights from airborne laser scanner data. *Forest Science*, **45**, pp. 407–422.

McCombs, J.W., Roberts, S.D. and Evans, D.L., 2003, Influence of fusing LiDAR and multispectral imagery on remotely sensed estimates of stand density and mean tree height. *Forest Science*, **49**, pp. 457–466.

Morsdorf, F., Meier, E., Allgower, B. and Nuesch, D., 2003, Clustering in airborne laser scanning raw data for segmentation of single trees. *International Archives of the Photogrammetry, Remote Sensing and Spatial Information Sciences*, **34**, pp. 27–33.

Nilsson, M., 1996, Estimation of tree heights and stand volume using an airborne LiDAR system. *Remote Sensing of Environment*, **56**, pp. 1–7.

Persson, A., Holmgren, J. and Soderman, U., 2002, Detecting and measuring individual trees using an airborne laser scanner. *Photogrammetric Engineering and Remote Sensing*, **68**, pp. 925–932.

Popescu, S.C. and Wynne, R.H., 2004, Seeing the trees in the forest: using lidar and multispectral data fusion with local filtering and variable window size for estimating tree height. *Photogrammetric Engineering and Remote Sensing*, **70**, pp. 589–604.

Popescu, S.C., Wynne, R.H. and Nelson, R.F., 2003, Measuring individual tree crown diameter with lidar and assessing its influence on estimating forest volume and biomass. *Canadian Journal of Remote Sensing*, **29**, pp. 564–577.

Popescu, S.C., Wynne, R.H. and Scrivani, J., 2004, Fusion of small-footprint lidar and multispectral data to estimate plot-level volume and biomass in deciduous and pine forests in Virginia, USA. *Forest Science*, **50**, pp. 551–565.

Popescu, S.C. and Zhao, K., 2008, A voxel-based lidar method for estimating crown base height for deciduous and pine trees. *Remote Sensing of Environment*, **112**, pp. 767–781.

Pyysalo, U. and Hyyppä, H., 2002, Reconstructing tree crowns from laser scanner data for feature extraction. *International Society for Photogrammetry and Remote Sensing – ISPRS Commission III, Symposium 2002*, 9–13 September, Graz, Austria, pp. B–218.

Reutebuch, S., Andersen, H. and McGaughey, R., 2005, Light detection and ranging (LIDAR): an emerging tool for multiple resource inventory. *Journal of Forestry*, **103**, pp. 286–292.

ROTH, B.E., JOKELA, E.J., MARTIN, T.A., HUBER, D.A. and WHITE, T.L., 2007*a*, Genotype × environment interactions in selected loblolly and slash pine plantations in the Southeastern United States. *Forest Ecology and Management*, **238**, pp. 175–188.

ROTH, B.E., SLATTON, K.C. and COHEN, M.J., 2007*b*, On the potential for high-resolution lidar to improve rainfall interception estimates in forest ecosystems. *Frontiers in Ecology and the Environment*, **5**, pp. 421–428.

SCHARDT, M., ZIEGLER, M., WIMMER, A., WACK, R. and HYYPPÄ, R., 2002, Assessment of forest parameter by means of laser scanning. *International Archives of the Photogrammetry, Remote Sensing and Spatial Information Sciences*, **34**, pp. 302–309.

SHRESTHA, R.L., CARTER, W.E., LEE, M., FINER, P. and SARTORI, M., 1999, Airborne laser swath mapping: accuracy assessment for surveying and mapping applications. *Journal of American Congress on Surveying and Mapping*, **59**, pp. 83–94.

SLATTON, K.C., CARTER, W.E., SHRESTHA, R.L. and DIETRICH W., 2007, Airborne laser swath mapping: achieving the resolution and accuracy required for geosurficial research. *Geophysical Research Letters*, **34**, L23S10.

SONG, C., 2007, Estimating tree crown size with spatial information of high resolution optical remotely sensed imagery. *International Journal of Remote Sensing*, **28**, pp. 3305–3322.

SPRINZ, P.T. and BURKHART, H.E., 1987, Relationships between tree crown, stem, and stand characteristics in unthinned loblolly pine plantations. *Canadian Journal of Forest Research*, **17**, pp. 534–538.

SWINDEL, B.F., NEARY, D.G., COMERFORD, N.B., ROCKWOOD, D.L. and BLAKESLEE, G.M., 1998, Fertilization and competition control accelerate early southern pine growth on flatwoods. *Southern Journal of Applied Forestry*, **12**, pp. 116–121.

WACK, R., SCHARDT, M., LOHR, U., BARRUCHO, L. and OLIVEIRA, T., 2003, Forest inventory for eucalyptus plantations based on airborne laser scanner data. *International Archives of Photogrammetry, Remote Sensing, and Spatial Information Sciences*, **34**, pp. 40–46.

WEED, C.A., CRAWFORD, M.M., NEUENSCHWANDER, A.L. and GUTIERREZ, R., 2002, Classification of LiDAR data using a lower envelope follower and gradient based operator. *Proceedings of the IEEE International Geoscience Remote Sensing Symposium (IGARSS '02)*, **3**, pp. 1384–1386.

ZHANG, K., CHEN, S., WHITMAN, D., YAN, J. and ZHANG, C., 2003, A progressive morphological filter for removing nonground measurements from airborne LIDAR data. *IEEE Transactions on Geoscience and Remote Sensing*, **41**, pp. 872–882.